Acta Cryst. (1966). **20**, 268

The Crystal Structures of WTe_2 and High-Temperature $MoTe_2$

BRUCE E. BROWN*

Research Division, Allis-Chalmers Manufacturing Company, Milwaukee 1, *Wisconsin, U.S.A.*

(*Received* 2 *November* 1964 *and in revised form* 30 *June* 1965)

The structures of WTe_2 and a high-temperature monoclinic polymorph of $MoTe_2$ have been solved by Patterson methods. Single crystals were grown by vapor transport methods. Cell dimensions, as measured on precession photographs, are for WTe_2, $a=6{\cdot}282$ Å, $b=3{\cdot}496$ Å, $c=14{\cdot}07_3$ Å. Similarly for $MoTe_2$, $a=6{\cdot}33$ Å, $b=3{\cdot}469$ Å, $c=13{\cdot}86$ Å, $\beta=93°55'$. Intensities were measured for both crystals from zero- and first-level Weissenberg photographs. WTe_2 and $MoTe_2$ are given the space groups $Pnm2_1$ and $P2_1/m$, respectively. Minimum function maps prepared by a superposition method gave approximate trial structures for both compounds which were refined by least-squares methods to R values of 12·5 % and 13·9 % for WTe_2 and $MoTe_2$ respectively. Both compounds are layer structures with double sheets of tellurium atoms bound together by interleaving metal atoms. An off-center positioning of metal atoms in the tellurium octahedra buckles the tellurium sheets and allows metal atoms in adjacent octahedra to approach each other. Each metal atom, therefore, has eight neighbors, six tellurium atoms and two metal atoms, and a significant amount of metal–metal bonding is introduced.

Introduction

The structure of tungsten ditelluride was first thought to be of the *C*7 (MoS_2) type (Goldschmidt, 1919). Knop & Haraldsen (1956) showed that this was not the case, although they thought it probable that the structure was closely related to the *C*7 type. The present investigation shows WTe_2 to be a layer structure, as is the *C*7 type, but with a distorted octahedral coordination about the tungsten atom. Therefore, the compound is geometrically more closely related to the CdI_2 (*C*6) type.

Puotinen & Newnham (1961) reported the structure of $MoTe_2$ to be the *C*7 type. Work in this laboratory has shown that the *C*7 form of $MoTe_2$ is the stable form below *ca.* 900°C, but that a different polymorphic type forms above this temperature. The structural study reported here shows this high temperature type to be effectively isostructural with WTe_2. Different symmetries in the two compounds arise largely from small differences in layer stacking.

Experimental

Excellent single crystals of tungsten and molybdenum tellurides were prepared by vapor transport methods (Nitsche, Bolsterli & Lichtensteiger, 1961) using bromine as the transporting agent for molybdenum and tungsten. The crystals adopt a rod or lath-shaped habit with the shortest crystallographic axis (*b*) parallel to the long dimension of the lath. Chemical analysis of the transported material gave for the tungsten compound, 39·2% tungsten and 57·7% tellurium by weight, and for the molybdenum compound 26·7% molybdenum and 72·2% tellurium by weight. These figures are equivalent to the formulas $W_{0.94}Te_2$ and $Mo_{0.985}Te_2$ respectively, where two tellurium atoms have been assumed for each formula.

The unit-cell dimensions as measured from precession photographs with Mo $K\alpha$ radiation are: for WTe_2, $a=6{\cdot}282$, $b=3{\cdot}496$, $c=14{\cdot}07_3$ Å; and for $MoTe_2$, $a=6{\cdot}33$, $b=3{\cdot}469$, $c=13{\cdot}86$ Å, $\beta=93°55'$.

Measured densities for WTe_2 and $MoTe_2$ are 9·51 $g.cm^{-3}$ and 7·5 $g.cm^{-3}$ respectively. Both of these values indicate four MX_2 units per cell corresponding to the theoretical densities, 9·44 $g.cm^{-3}$ and 7·67 $g.cm^{-3}$ for WTe_2 and $MoTe_2$ respectively. The axial designation used for WTe_2 in this study is altered from that used by Knop & Haraldsen (1956), *a* and *b* being interchanged. This change allows orthorhombic WTe_2 and monoclinic $MoTe_2$ to be described by similar axes where $MoTe_2$ conforms to the customary (second) setting having the *b* axis as the unique axis.

For both compounds $0kl$ reflections are absent when $k+l$ is odd. The possible space groups for WTe_2 are then *Pnmm* and $Pnm2_1$; for $MoTe_2$ however, these absences must be accidental, indicating a pseudo *n*-glide. Refinement of the structure indicated the correct space group to be $P2_1/m$. Zero- and upper-level Weissenberg photographs of both crystals were taken using the short (*ca.* 3·5 Å) *b* axis as the rotation axis. In each case, the distribution of intensities was identical on all even layer photographs; the odd-layer photographs were similarly identical. Accordingly, all atoms must lie on mirror planes separated by $\frac{1}{2}$ in *y*. Intensities on the zero- and first-layer photographs were estimated visually by comparison with a standard intensity scale; they were corrected for Lorentz and polarization effects, absorption, spot extension on upper layers (Phillips, 1954) and α_1–α_2 splitting (Brown, 1965). There were 220 $h0l$ and 212 $h1l$ observed WTe_2 reflections,

---

* Present address: Geology Department, University of Wisconsin-Milwaukee, Milwaukee, Wisconsin, U.S.A.

and 243 $h0l$ and 260 $h1l$ observed $MoTe_2$ reflections (Table 5). Additional higher odd and even levels were calculated by scaling the $h0l$ and $h1l$ levels according to the scattering factor decline with increasing $\sin\theta/\lambda$. These additional levels were needed for the calculation of Harker sections.

The correct space group and approximate structure of WTe_2 were deduced from Patterson sections. The section $u0w$ had no peaks located on the z axis, indicating the absence of a twofold axis parallel to x; the correct space group is thus $Pnm2_1$. The twelve atoms in the cell (four WTe_2 units) must occupy six sets of twofold positions, each atom being related to its equivalent atom by the vector $2x, \frac{1}{2}, \frac{1}{2}$, through the n-glide operation. Four peaks were present on the Harker line $u, \frac{1}{2}, \frac{1}{2}$, two weak and two strong. The height of the origin peak and the heights of several suspected W–Te peaks on the $u0w$ and $u\frac{1}{2}w$ sections indicated that the strong peaks were due to W–W vectors and the weak peaks to doubled Te–Te vectors. The W–W vectors were used as the translation vectors in the minimum-function superposition method (Buerger, 1959, p.260) and a trial structure was obtained. There were ambiguities with regard to some of the tellurium atoms, but by consideration of the configuration of the shortest W–Te vectors and related Te–Te vectors it was possible to eliminate the superfluous peaks.

The $MoTe_2$ structure is isostructural with WTe_2 even though there are symmetry differences. This was suspected initially because of the similarity in the lattice parameters and systematic absences. Molybdenum–molybdenum vectors were identified by analogy to the WTe_2 structure and a correct trial structure was deduced from a minimum-function superposition.

Refinements of both structures were carried out with the full-matrix least-squares program of Busing & Levy (1959) for the IBM 704 computer. The scattering factors of Thomas & Umeda (1957) were used for both structures. The reflections were weighted according to the relation $w^{\frac{1}{2}}=1/0{\cdot}1(|F_o|)$. Very weak reflections were given reduced weight and unobserved reflections were given zero weight.

In the first WTe_2 cycle only the scale factor for each layer was varied. The two scale factors were fixed in remaining cycles. The maximum positional parameter shift on the last cycle was $1{\cdot}4\sigma$ (0·009 Å), although nine of the eleven variable positional parameters were less than 1σ and the average shift was $0{\cdot}6\sigma$. Several strong interactions were noted in the correlation coefficients (Geller, 1961). These are listed in Table 1. Pseudo centers of symmetry relating the pairs Te(1)–Te(4) and Te(2)–Te(5) may account for some of these interactions. The final R index and weighted R index are 12·5% and 15·9% respectively.

Table 2. *Refined parameters of* WTe_2 *and* $MoTe_2$

(σ) Applies to rightmost digit of quantity in question.

		WTe_2		
Atom	$x(\sigma_x)$	y	$z(\sigma_z)$	$B(\sigma_B)$
W(1)	0·9005(5)	$\frac{1}{2}$	0	0·12(4)
W(2)	0·5414(6)	0	0·9851(3)	0·14(4)
Te(1)	0·2941(10)	$\frac{1}{2}$	0·0965(5)	0·42(8)
Te(2)	0·8002(10)	0	0·1400(5)	0·55(8)
Te(3)	0·3559(11)	0	0·3449(5)	0·63(9)
Te(4)	0·8517(10)	$\frac{1}{2}$	0·3893(5)	0·45(8)
		$MoTe_2$		
Mo(1)	0·1833(8)	$\frac{1}{4}$	0·0074(3)	0·21(7)
Mo(2)	0·3181(8)	$-\frac{1}{4}$	0·5066(3)	0·23(7)
Te(1)	0·5888(6)	$\frac{1}{4}$	0·1045(3)	0·28(6)
Te(2)	0·0970(6)	$-\frac{1}{4}$	0·1486(3)	0·48(6)
Te(3)	0·5568(6)	$-\frac{1}{4}$	0·3516(3)	0·41(6)
Te(4)	0·0563(6)	$\frac{1}{4}$	0·3955(3)	0·33(6)

The $MoTe_2$ structure was refined in two stages. During the first stage the space group Pm was mistakenly assumed because an origin similar to that in WTe_2 was chosen. The structure refined in ten cycles to an R of 12·9%. However, the temperature factors behaved badly, giving evidence of interaction, and the standard deviations were rather high. Dr Richard E. Marsh then pointed out that the resulting structure had an arrangement fitting the symmetry $P2_1/m$ very closely.

Three refinement cycles based on this space group produced an R value of 13·9% and a weighted R index of 16·4%, but the temperature factors behaved normally and the standard deviations were reduced by a factor of five. During the final cycle the largest positional parameter shifts were less than 0·3 of a standard deviation and the correlation matrix showed no strong interactions. This is additional evidence that the interactions observed in WTe_2 are arising as a consequence of the pseudo symmetry.

Description of the structure

Both of these compounds are layer structures with molybdenum or tungsten atoms binding two sheets of tellurium atoms into infinite two-dimensional layers; binding between the layers is through Te–Te contacts

Table 1. *Correlation coefficients of the stronger* WTe_2 *interactions*

B refers to temperature factor – temperature factor interactions, Z to Z–Z parameter interactions. These were the only large correlations. All ϱ_{ij} multiplied by 10^2.

	W(1)	W(2)	Te(1)	Te(2)	Te(3)	Te(4)
W(1)		$-58B$		$-40B$		
W(2)						
Te(1)				$-20B$	$17B$	$-52B$, $54Z$
Te(2)					$-52B$, $56Z$	$10B$
Te(3)						$-27B$

only. In the sulfide and selenide layer structures of molybdenum and tungsten, the metal atoms are coordinated by anions located at the corners of trigonal prisms, but in these two structures the metal atoms are coordinated by anions at the corners of distorted octahedra. Figs. 1 and 2 illustrate the nature of this distortion. The metal atoms are not located in the centers of the octahedra, and the distortion of the octahedra buckles the tellurium atom layers. The off-center position of the metal atoms together with the buckling of the tellurium layers gives the structure a definite ribbon-like aspect and is presumably responsible for the rod- or lath-like appearance of the crystals instead of the platy habit usually associated with layer compounds. The stacking of one layer upon another is governed by the buckling of the layers so that adjacent layers are keyed together by an association of ripples and troughs. There may be other factors controlling stacking, however, for slight differences in the placement of one layer upon its neighbor are responsible for the difference in symmetry between $MoTe_2$ and WTe_2 (compare Figs. 1 and 2). This difference in stacking is not an apparent result of configuration differences in individual compound layers since the configuration of an individual WTe_2 layer is very nearly identical with an individual $MoTe_2$ layer.

Metal—metal bonding

The asymmetry of the metal positions changes the near-neighbor coordination of the metal atoms from six to eight because two metal-atom neighbors are at about the same distance as the six tellurium atoms. The metal–metal neighbors coordinate into linked zigzag chains parallel to *y* (Fig. 3) and metal–metal bonding is probably present in a significant degree.

The phenomenon of metal–metal bonding, prominent in these two structures, is a common phenomenon among transition metal oxides in which the oxidation state of the metal is not at a maximum (Marinder & Magnéli, 1957, Marinder, Dorm & Seleborg, 1962). It has also been observed in Mo_2S_3 (Jellinek, 1961). These telluride structures are an example of the same phenomenon but are more closely related to the Mo_2S_3 structure than to any of the oxides.

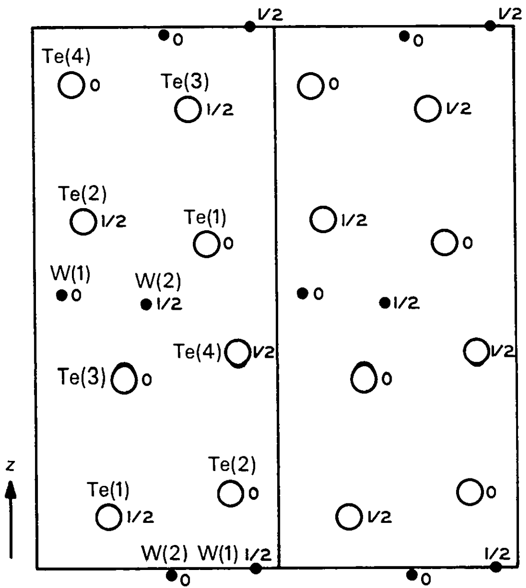

Fig. 1. A projection of the WTe_2 structure onto the (010) face. Large open circles: tellurium atoms; small filled circles: tungsten atoms. The designation 0 or $\frac{1}{2}$ refers to the *y* coordinate.

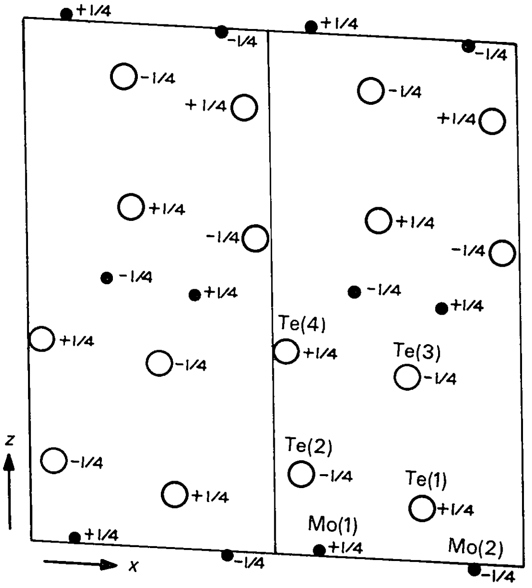

Fig. 2. A projection of the $MoTe_2$ structure onto the (010) face. Large open circles: tellurium atoms; small filled circles: molybdenum atoms. The designation $+\frac{1}{4}$ or $-\frac{1}{4}$ refers to the *y* coordinate.

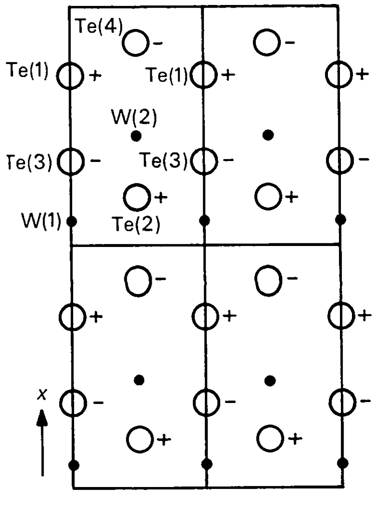

Fig. 3. Projection of a single WTe_2 compound layer onto the (001) face. The tungsten atoms (small filled circles) in the plane of the page. The tellurium atoms (large open circles) are above (+) or below (−) the plane of the page.

In $MoTe_2$ the Mo–Mo distance is 2·90 Å, which is 0·18 Å longer than in elementary molybdenum. In WTe_2 the W–W distance of 2·86 Å is 0·13 Å longer than in elementary tungsten. The shorter metal–metal distances in WTe_2 may tend to stabilize WTe_2 relative to $MoTe_2$ and may partially explain why a *C*7 form of WTe_2 has not been observed while a *C*7 form of $MoTe_2$ can be easily made.

It is also probable that the metal–metal bonding observed in the high-temperature form of $MoTe_2$ is responsible for its high electrical conductivity (10^3 ohm^{-1}cm^{-1}) relative to the *C*7-type $MoTe_2$ (10^{-3} ohm^{-1}cm^{-1}). WTe_2 is likewise a good conductor.

Table 3. *Bond distances for* WTe_2 *and* $MoTe_2$ (Å)

WTe_2

Atom 1–atom 2		$d(\sigma_d)$	Atom 1–atom 2		$d(\sigma_d)$
M–M distances			X–X distances parallel to layering		
W(1)	W(2)	2·861(4)	Te(1)	Te(2)	3·679(8)
M–X distances in octahedron 1					
W(1)	Te(1)	2·820(7)	Te(1)	Te(2)	3·613(8)
W(1)	Te(2)(2)	2·708(5)	Te(3)	Te(4)	3·625(8)
W(1)	Te(3)	2·713(8)	Te(3)	Te(4)	3·671(8)
W(1)	Te(4)(2)	2·811(6)	Te(*i*)	Te(*i*)	3·496*
M–X distances in octahedron 2			X–X distances between layers		
W(2)	Te(1)(2)	2·814(6)	Te(1)	Te(3)	3·927(8)
W(2)	Te(2)	2·720(7)	Te(2)	Te(4)	3·932(8)
W(2)	Te(3)(2)	2·713(6)			
W(2)	Te(4)	2·813(7)	X–X distances across layers		
			Te(1)	Te(4)	3·520(6)

* Equal to the *b*-axis length.

Table 3 (*cont.*)

$MoTe_2$

M–M distances			X–X distances parallel to layering		
Mo(1)	Mo(1)	2·895(8)	Te(1)	Te(2)	3·652(5)
Mo(2)	Mo(2)	2·901(9)	Te(1)	Te(2)	3·671(5)
M–X distances in octahedron 1					
Mo(1)	Te(1)	2·816(7)	Te(3)	Te(4)	3·700(5)
Mo(1)	Te(2)(2)	2·701(6)	Te(3)	Te(4)	3·622(5)
Mo(1)	Te(1)	2·793(5)	Te(*i*)	Te(*i*)	3·469*
Mo(1)	Te(2)(2)	2·698(5)			
			X–X distances between layers		
M–X distances in octahedron 2			Te(2)	Te(3)	3·908(6)
Mo(2)	Te(4)	2·811(7)	Te(2)	Te(4)	3·859(5)
Mo(2)	Te(3)(2)	2·699(5)	Te(3)	Te(1)	3·855(5)
Mo(2)	Te(3)	2·710(7)			
Mo(2)	Te(4)(2)	2·789(5)	X–X distances across layers		
			Te(4)	Te(4)	3·493(7)

Table 4. *Bond angles* (°) *for* WTe_2 *and* $MoTe_2$

WTe_2

Angle (σ)		Angle (σ)	
X–M–X angles in octahedron 1		X–M–X angles in octahedron 2	
Te(1)–W(1)–Te(2)	81·6(2)	Te(2)–W(2)–Te(1)	83·3(2)
Te(1)–W(1)–Te(4)	77·4(2)	Te(2)–W(2)–Te(3)	116·2(2)
Te(3)–W(1)–Te(2)	116·6(2)	Te(4)–W(2)–Te(1)	77·4(2)
Te(3)–W(1)–Te(4)	83·3(2)	Te(4)–W(2)–Te(3)	81·9(2)
Te(2)–W(1)–Te(4)	97·6(1)	Te(1)–W(2)–Te(3)	97·9(1)
Te(2)–W(1)–Te(2)	80·3(2)	Te(1)–W(2)–Te(1)	76·7(2)
Te(4)–W(1)–Te(4)	76·8(2)	Te(3)–W(2)–Te(3)	80·2(2)
X–X–X angles parallel to layering		X–X–X angles across layering	
Te(1)–Te(2)–Te(1)	56·7(1)	Te(1)–Te(3)–Te(1)	52·8(1)
Te(2)–Te(1)–Te(2)	118·9(2)	Te(2)–Te(4)–Te(2)	52·7(1)
Te(3)–Te(4)–Te(3)	57·6(1)	Te(1)–Te(4)–Te(1)	59·5(1)
M–M–M angles			
W(1)–W(2)–W(1)	75·2(1)		

$MoTe_2$

X–M–X angles in octahedron 1		X–M–X angles in octahedron 2	
Te(1)–Mo(1)–Te(2)	82·9(2)	Te(4)–Mo(2)–Te(3)	82·2(2)
Te(2)–Mo(1)–Te(2)	80·0(2)	Te(4)–Mo(2)–Te(4)	77·2(2)
Te(2)–Mo(1)–Te(1)	98·1(1)	Te(4)–Mo(2)–Te(4)	76·9(2)
Te(2)–Mo(1)–Te(2)	115·2(2)	Te(4)–Mo(2)–Te(3)	97·8(1)
Te(2)–Mo(1)–Te(1)	83·8(2)	Te(3)–Mo(2)–Te(4)	84·6(2)
Te(1)–Mo(1)–Te(1)	77·0(2)	Te(3)–Mo(2)–Te(3)	115·2(2)
X–X–X angles parallel to layering		X–X–X angles across layering	
Te(1)–Te(2)–Te(1)	56·7(1)	Te(2)–Te(4)–Te(2)	53·4(1)
Te(1)–Te(2)–Te(1)	119·7(1)	Te(3)–Te(1)–Te(3)	53·5(1)
		Te(4)–Te(4)–Te(4)	59·5(1)
M–M–M angles			
Mo(1)–Mo(1)–Mo(1)	73·6(2)		
Mo(2)–Mo(2)–Mo(2)	73·5(3)		

Table 5. F_o and F_c for WTe_2

ℓ	fo	fc	A	B
00ℓ				
4	88	48	-47	-8
6	262	234	224	67
8	309	330	308	120
10	224	177	159	76
12	196	172	145	91
14	148	123	95	77
16	0	6	4	4
18	105	102	69	75
20	196	199	120	159
22	0	49	27	41
24	65	56	-25	-49
26	0	39	11	37
28	85	82	24	79
10ℓ				
4	62	45	-28	35
5	250	235	-55	228
6	114	79	-36	-70
7	271	237	-51	231
8	234	183	53	-175
9	113	86	57	-63
10	111	79	56	-55
11	93	70	34	-61
12	0	17	-17	5
13	205	189	-104	158
14	112	99	27	-96
15	156	148	-71	130
16	167	152	97	-117
17	50	39	39	-4
18	83	88	70	-54
19	0	12	12	1
20	58	68	53	-43
21	0	46	-29	35
22	89	87	73	-48
23	0	30	-12	27
24	53	77	67	-37
25	0	43	-30	30
26	76	85	76	-38
27	0	38	-27	27
28	85	101	98	-25
20ℓ				
0	43	39	-39	0
1	203	196	195	17
2	197	178	137	113
3	235	209	170	122
4	352	289	282	64
5	153	126	-110	62
6	172	136	136	-2
7	50	40	-37	15
8	72	52	35	38
9	137	108	83	68
10	129	101	66	76
11	94	76	43	62
12	93	82	51	63
13	110	97	62	74
14	96	93	38	85
15	139	123	60	107
16	130	119	68	97
17	42	38	-20	32
18	44	44	33	29
19	32	12	7	9
20	34	38	-38	0
21	137	140	78	116
22	51	72	-30	65
23	117	126	34	121
24	75	84	15	83
25	0	26	-13	23
26	0	17	5	16
27	0	30	9	28
28	0	32	-29	-12
29	0	86	20	84
30	62	34	-32	12
30ℓ				
0	129	125	-125	0
1	218	204	-21	202
2	115	121	-120	-14
3	190	192	21	191
4	180	171	-75	-154
5	174	164	30	161
6	102	85	-79	-32
7	169	160	-112	113
8	199	195	-149	125
9	191	177	-127	123
10	112	99	-76	-64
11	169	168	7	167
12	196	201	38	-197
13	122	117	8	117
14	38	52	-32	-40
15	79	88	-83	31
16	93	101	-95	31
17	84	91	-80	43
18	55	52	-14	-50
19	75	84	-35	76
20	60	71	23	-67
21	51	57	-29	49
22	0	37	3	-37
23	53	40	-25	31
40ℓ				
0	102	95	-95	0
1	133	143	-124	-71
2	140	147	-13	-146
3	105	100	-100	-1
4	27	31	17	26
5	130	130	127	29
6	144	139	-71	119
7	129	121	121	-10
8	70	67	-61	27
9	23	32	27	-16
10	24	30	-24	17
11	61	51	49	15
12	58	54	-47	26
13	47	46	46	2
14	40	31	-31	2
15	42	33	29	17
16	61	69	-41	55
17	111	124	84	90
18	111	127	-101	76
19	115	121	95	75
20	72	66	-65	2
21	0	23	23	-5
22	0	8	-1	-8
23	0	23	0	23
24	0	64	-50	39
25	101	110	37	104
26	85	102	-98	29
27	75	95	44	84
50ℓ				
0	123	111	-111	0
1	97	95	-6	95
2	149	152	-152	0
3	137	136	-73	114
4	140	133	-127	40
5	84	78	-73	27
6	0	22	-21	5
7	47	50	35	36
8	115	113	-71	-88
9	143	134	-22	132
10	182	192	-183	-58
11	163	159	-150	51
12	129	127	-117	48
13	101	97	-83	-51
14	42	31	-9	29
15	0	14	-3	13
16	65	68	-35	-58
17	75	73	-55	48
18	92	99	-86	-49
19	72	77	-76	-14
20	63	66	-66	0
21	37	60	-49	-35
22	0	46	-46	-4
23	38	55	-46	-31
24	38	45	-45	-7
60ℓ				
0	0	24	24	0
1	0	25	22	-12
2	84	89	-74	49
3	220	240	58	-232
4	146	143	-143	-5
5	203	209	43	-205
6	63	60	-52	-29
7	52	53	12	-51
8	27	23	-23	0
9	73	76	45	-61
10	64	65	-65	5
11	86	103	68	-77
12	74	60	-58	16
13	70	72	57	-43
14	65	62	-60	11
15	94	117	89	-76
16	69	75	-68	-31
17	94	110	82	-72
18	0	31	-28	-13
19	0	13	2	13
20	0	44	-22	38
21	0	31	11	28
22	54	63	-62	10
23	93	95	92	-20
24	66	63	-55	-32
25	65	67	64	-19
70ℓ				
0	0	1	1	0
1	0	9	8	-2
2	27	37	37	1
3	0	22	-14	-16
4	0	20	-17	10
5	69	59	-58	11
6	131	120	-118	-17
7	41	45	-42	17
8	0	7	0	7
9	43	46	-18	-43
10	132	130	107	72
11	85	84	-54	-64
12	33	27	-21	16
13	89	85	-83	-20
14	139	115	-102	-52
15	50	60	-57	-18
16	0	20	-16	12
17	74	75	-38	-65
18	65	61	18	58
19	84	90	-48	-76
20	0	22	-16	15
21	66	74	-45	-59
22	0	24	-23	1
23	66	72	-34	-63
24	0	28	-28	1
25	74	82	-37	-73
80ℓ				
0	0	32	-32	0
1	210	212	18	-211
2	80	83	-20	80
3	61	51	13	-49
4	0	17	5	-16
5	54	51	3	-51
6	84	73	6	-73
7	170	150	44	-143
8	0	21	-16	-14
9	151	139	57	-126
10	0	12	-5	-10
11	98	103	45	-92
12	0	34	9	-33
13	96	90	50	-75
14	0	9	-5	-7
15	0	38	26	-27
16	0	24	16	-18
17	0	37	21	-31
18	76	73	50	-54
19	101	107	77	-74
20	0	31	13	-28
21	85	85	70	-47
22	37	16	-15	5
90ℓ				
0	88	73	73	0
1	0	18	-18	3
2	92	77	76	9
3	0	21	18	10
4	113	107	105	20
5	34	34	30	15
6	135	126	122	31
7	99	90	-87	-23
8	87	72	68	21
9	114	100	-93	-36
10	0	27	24	10
11	52	36	29	21
12	74	69	58	37
13	0	19	14	13
14	100	102	83	59
15	107	100	-79	-61
16	38	61	49	36
17	76	83	-62	-55
10.0ℓ				
0	0	10	10	0
1	0	35	18	-30
2	146	116	18	-115
3	0	31	23	-21
4	0	22	10	-19
5	0	36	4	-36
6	74	44	0	44
7	0	38	9	-37
8	0	34	21	-27
9	0	20	17	-9
10	65	62	31	-54
11	0	21	21	-4
12	76	56	34	-44
13	0	38	34	-15
14	101	85	59	-61
15	0	32	30	-9
16	54	52	39	-33
17	0	11	10	-3
18	0	5	5	0
19	0	14	14	0
20	73	69	59	-37
21	0	30	27	14
22	104	124	107	-61
11.0ℓ				
0	119	105	105	0
1	37	44	-1	44
2	92	81	81	0
3	38	45	-32	31
4	100	82	82	0
5	38	53	-35	40
6	132	117	110	39
7	85	74	34	65
8	101	91	70	58
9	54	56	34	44
10	0	40	35	18
11	66	50	-50	0
12	76	76	74	18
13	66	57	-55	14
14	100	94	73	58
15	53	57	11	56
16	37	55	22	50
12.0ℓ				
0	76	68	-68	0
1	108	85	-18	83
2	0	44	-32	30
3	0	13	-13	2
4	0	5	3	-5
5	0	23	14	18
6	76	53	-15	-50
7	85	71	7	71
8	76	54	-28	-46
9	65	50	0	50
18	57	63	33	-53
20	44	49	6	-48
01ℓ				
5	252	192	-45	187
7	134	100	30	-95
9	118	82	32	-75
11	277	257	-126	223
13	243	229	-129	189
15	0	16	10	-12
17	0	24	-20	13
19	163	150	-117	92
21	127	122	-100	70
23	97	103	-90	50
25	106	108	-100	39
27	0	50	-48	13
29	0	52	-51	10
31	0	126	-125	15
33	82	107	-107	4
35	59	31	-31	-2
11ℓ				
3	343	316	-315	-13
4	91	64	-8	-64
5	291	273	-257	-91
6	256	202	-182	-87
7	164	129	-112	-62
8	55	37	-22	-29
9	169	137	-125	-55
10	37	28	15	-24
11	157	144	-122	-75
12	53	42	-14	-39
13	122	106	-87	-60
14	0	27	26	-6
15	155	131	-101	-83
16	76	56	-21	-52
17	147	122	-68	-100
18	166	145	-86	-116
19	0	36	-4	-36
20	0	32	-17	-27
21	0	24	-18	-16
22	72	59	40	43
23	74	82	-42	-70
24	0	50	-4	-50
25	65	62	-9	-62
26	84	108	-34	-103
21ℓ				
0	210	167	0	-167
1	86	76	73	21
2	258	235	21	-234
3	109	93	91	-21
4	191	164	53	-155
5	58	41	29	-28
6	26	18	-17	2
7	155	129	-30	125
8	173	150	-8	-149
9	184	160	34	156
10	283	288	114	-264
11	105	90	89	9
12	115	98	68	-71
13	0	16	5	-15
14	53	44	-40	18
15	137	117	-74	91
16	109	93	21	-90
17	133	113	-36	107
18	149	131	79	-104
19	47	48	-3	48
20	48	53	32	-43
21	35	43	-29	32
22	36	38	19	-33
23	52	53	-39	35
24	0	33	18	-27
25	0	48	-43	22
26	0	24	-12	-20
27	53	73	-69	23
28	0	38	13	-35
29	51	67	-60	30
31ℓ				
0	163	172	0	-172
1	224	216	-214	-29
2	64	58	-49	-31
3	127	115	114	-14
4	115	97	-53	81
5	82	80	80	1
6	28	33	-15	-30
7	139	124	-109	-59
8	97	89	-17	-88
9	93	83	-54	-63
10	82	75	-54	-51
11	49	51	1	-51
12	92	83	-53	-64
13	73	71	-9	-71
14	83	82	-58	-58
15	58	57	54	-19
16	85	79	-75	-25
17	63	55	55	-1
18	73	68	-31	-60
19	107	99	-22	-96
20	117	106	4	-106
21	89	91	3	-91
22	90	93	-45	-81
23	64	76	72	24
24	65	85	-69	-49
25	37	59	56	19
26	0	62	-14	-60
27	37	61	23	-56
28	52	76	12	-75
41ℓ				
0	139	142	0	-142
1	114	110	108	18
2	111	94	2	-94
3	101	89	89	-1
4	140	146	56	-134
6	259	250	80	-237
7	175	187	170	78
8	125	117	12	-116
9	0	27	1	27
10	25	33	-4	33
11	52	45	31	-31
12	121	111	94	-58
13	169	159	148	56
14	203	191	122	-148
15	125	127	89	90
16	70	70	36	-60
17	0	16	13	10
18	0	17	13	11
19	35	32	32	0
20	51	52	51	-9
21	36	49	38	31
51ℓ				
0	192	206	0	206
1	166	164	139	-87
2	132	135	-111	77
3	95	92	16	-90
4	23	20	-7	-18
5	33	43	-1	43
6	84	78	17	76
7	93	91	83	35
8	129	122	-76	95
9	102	103	98	-32
10	86	89	-76	46
11	69	67	65	-17
12	77	73	-63	38
13	79	78	74	-24
14	69	76	-76	-9
16	47	43	-31	-29
17	0	21	20	-6
19	81	65	54	35
20	82	96	-95	14
21	74	111	110	-13
22	75	87	-61	-62
61ℓ				
0	35	42	0	-42
1	84	86	86	-10
2	44	43	15	-40
3	72	70	66	23
4	73	65	-53	-36
5	37	41	26	32
6	46	38	38	-2
7	77	78	60	-50
8	186	174	171	31
9	115	115	111	-31
10	78	67	62	-23
11	96	80	55	58
12	93	70	-44	-54
13	0	24	10	22
14	57	66	53	39
15	68	72	57	-44
16	149	148	119	87
17	51	73	72	-9
18	36	70	63	29
19	0	47	41	23
20	0	38	33	18
21	37	38	38	6
22	37	63	38	51
71ℓ				
0	178	171	0	171
1	143	120	43	112
2	160	145	38	140
3	127	107	20	105
4	128	113	-22	111
5	96	90	56	-70
6	164	147	-72	128
7	90	77	61	-46
8	155	133	-48	124
9	31	40	19	35
10	110	98	-37	91
11	32	31	22	21
12	106	103	-55	87
13	34	41	15	37
14	105	102	-51	88
15	36	36	1	36
16	36	67	-47	48
17	37	62	54	-30
18	37	67	-64	22
19	37	56	53	-17
20	37	70	-55	43
21	37	60	-37	48
81ℓ				
0	0	9	0	9
1	44	51	-51	0
2	31	27	26	5
3	0	19	-17	-8
4	89	82	80	18
5	84	82	-77	-29
6	0	25	15	20
7	104	97	-93	-26
8	57	52	-50	-11
9	0	9	5	7
10	59	56	52	21
11	35	19	17	-10
12	190	150	124	83
13	96	87	-61	-62
14	36	64	42	47
15	64	65	-51	-40
16	0	4	0	3
17	0	6	5	3
18	37	61	40	46
19	37	16	3	-15
20	84	94	52	78
21	37	32	-9	-31
22	37	80	40	69
91ℓ				
0	0	33	0	-33
1	48	33	-1	-33
2	102	83	-7	82
3	0	29	-4	-29
4	196	175	-32	172
5	0	43	-19	39
6	93	72	-21	69
7	35	59	-24	54
8	0	25	-13	21
9	36	34	-16	30
10	73	69	-34	60
11	0	26	-16	20
12	37	52	-28	44
13	0	28	-21	18
14	53	55	-34	42
15	65	45	-34	30
16	92	96	-68	67
17	75	77	-57	52
18	0	37	-30	21
19	52	67	-53	42
20	0	27	20	-19
21	0	28	-24	13
22	0	33	-30	14
23	0	35	-32	12
24	58	76	-69	31
25	56	69	-65	24
10.1ℓ				
0	0	31	0	-31
1	141	118	-118	-8
2	0	35	-10	-34
3	155	129	-128	-19
4	36	23	10	-20
5	36	48	-48	-6
6	0	21	21	-3
7	0	39	-38	-9
8	0	27	17	-21
9	175	157	-144	-62
10	0	42	27	-32
11	164	144	-128	-65
12	0	25	23	-8
13	0	13	-13	-3
14	0	11	9	5
15	0	17	-13	-10
16	0	22	22	0
17	91	95	-70	-64
18	0	35	35	4
19	62	76	-55	-53
11.1ℓ				
0	65	63	0	63
1	0	31	-15	-26
2	0	18	14	-10
3	0	25	24	-6
4	84	90	4	-80
5	53	54	13	52
12.1ℓ				
3	53	61	-56	-22
4	65	65	-26	-59
5	99	88	-77	-41
6	65	61	3	-61
7	74	74	-73	-13
12	72	76	-39	-65
13	71	77	-36	-68

Table 6. *F_o and F_c for* $MoTe_2$

ℓ	fo	fc
	00ℓ	
-4	23.4	-24.2
-6	17.5	20.0
-8	25.4	34.7
-10	15.4	13.1
-12	15.5	14.4
-14	8.7	8.0
-16	9.0	-7.6
-18	9.0	10.4
-20	24.5	25.5
-22	.0	.4
-24	12.8	-13.3
-26	.0	6.0
-28	10.2	12.4
	10ℓ	
3	6.9	-2.9
4	11.7	9.0
5	25.8	30.4
6	7.9	-6.6
7	20.2	24.6
8	17.2	-21.7
9	19.9	-22.1
10	.0	-2.3
11	11.9	-12.0
12	8.8	8.3
13	22.8	27.0
14	10.3	-9.5
15	14.4	14.5
16	13.5	-15.4
17	9.6	-11.0
	20ℓ	
0	22.6	16.1
1	29.5	-35.9
2	23.0	-19.9
3	19.6	-19.7
4	25.9	-35.1
5	20.5	21.1
6	9.0	-7.2
7	5.0	4.2
8	.0	-.0
9	13.8	-12.4
10	9.2	-8.7
11	5.5	-4.5
12	6.7	-6.0
13	9.8	-10.3
14	8.4	-9.5
15	9.8	-9.6
16	11.9	-13.8
17	7.7	8.1
18	.0	-.0
19	.0	.8
20	.0	6.5
21	17.1	-19.5
22	7.9	-7.9
23	8.0	-9.3
	30ℓ	
0	.0	-1.6
1	21.1	-19.1
2	8.2	5.1
3	18.9	-16.1
4	23.4	22.6
5	13.5	-10.5
6	14.8	-10.2
7	16.3	-12.4
8	25.3	-28.2
9	18.7	-17.1
10	17.1	15.3
11	13.2	-12.2
12	22.7	28.3
13	.0	-4.8
14	8.9	-9.3
15	.0	-5.8
16	13.2	-14.7
17	8.0	-8.9
18	8.4	8.0
19	.0	-6.8
20	7.6	7.9
	40ℓ	
0	14.8	-12.8
1	29.0	-34.8
2	4.5	3.9
3	9.6	-8.0
4	8.2	6.0
5	24.5	28.3
6	8.1	-6.0
7	11.9	9.6
8	3.2	-3.7
9	.0	-2.9
11	5.2	4.6
12	.0	-2.7
13	.0	-.9
14	.0	.2
15	.0	4.5
16	.0	3.9
17	20.8	21.6
18	.0	-2.9
19	.0	8.3
20	.0	-4.6
21	8.0	-10.9
22	.0	3.3
23	.0	4.0
24	.0	3.4
25	16.8	19.0
	50ℓ	
0	.0	.1
1	18.8	16.6
2	10.0	6.9
3	16.2	15.1
4	14.0	11.9
5	6.4	-4.4
6	11.5	-9.3
7	8.4	6.7
8	15.1	-13.0
9	23.5	28.8
10	15.9	14.9
11	8.0	10.3
12	16.2	17.2
13	8.7	-9.2
14	9.1	-6.5
15	6.7	5.9
16	5.0	-6.7
17	15.2	15.0
18	.0	7.6
19	.0	4.2
20	.0	7.0
21	8.1	1.9
	60ℓ	
0	14.4	-12.7
1	13.6	-10.1
2	27.6	28.1
3	.0	-2.8
4	23.7	26.8
5	5.1	5.3
6	.0	-2.6
7	.0	.3
8	.0	1.3
9	4.1	-4.7
10	9.5	9.5
11	.0	-4.8
12	.0	3.8
13	.0	-4.7
14	9.9	12.0
15	.0	-1.3
16	10.7	13.3
	70ℓ	
0	.0	1.9
1	.0	3.9
2	.0	-.8
3	.0	-3.2
4	4.0	-5.3
5	21.8	-20.1
6	.0	-1.6
7	.0	.0
8	.0	-.9
9	22.9	20.8
10	6.6	-6.6
11	.0	-4.2
12	.0	-6.0
13	18.7	-21.2
18	8.2	-6.8
	80ℓ	
0	22.3	-22.4
1	13.9	13.1
2	4.4	4.9
3	.0	-3.5
4	.0	.9
5	10.3	-9.7
6	20.0	-17.3
7	.0	1.8
8	14.3	-13.3
10	5.1	-6.9
18	8.3	-14.4
	90ℓ	
0	.0	1.9
1	.0	-3.9
2	4.9	-5.2
3	7.1	-8.7
4	.0	-4.9
5	8.9	-11.1
6	13.9	14.6
7	.0	-1.1
8	10.8	9.9
9	.0	3.9
10	11.1	-12.1
11	.0	-6.4
12	.0	-3.2
13	10.0	-10.9
14	10.1	15.3
	10.0ℓ	
0	5.4	3.1
1	18.1	18.4
2	.0	3.7
3	.0	-4.4
4	.0	5.5
5	7.9	-10.0
13	5.9	7.8
	11.0ℓ	
0	.0	-.6
1	7.0	4.2
2	.0	-5.8
3	.0	7.4
4	.0	-1.2
5	11.6	12.1
6	11.7	12.0
7	.0	3.8
8	.0	2.9
9	.0	.1
10	10.3	-13.2
14	8.3	10.5
	10ℓ̄	
-3	8.4	-5.2
-4	11.3	-8.7
-5	23.4	26.5
-6	2.0	3.1
-7	25.4	30.9
-8	20.0	21.9
-9	17.3	-16.7
-10	7.4	6.1
-11	16.8	-17.0
-12	11.4	-9.1
-13	21.3	24.6
-14	7.1	6.4
-15	20.5	19.6
-16	16.5	16.3
-17	10.4	-8.4
	20ℓ̄	
-1	24.7	22.9
-2	9.7	-7.1
-3	28.8	32.6
-4	31.6	-36.4
-5	18.3	-14.1
-6	17.4	-14.8
-7	14.8	-12.3
-8	2.5	1.1
-9	12.9	11.0
-10	7.6	-7.0
-11	6.8	6.2
-12	5.6	-5.7
-13	7.7	7.9
-14	3.6	-6.2
-15	13.9	13.0
-16	15.3	-14.3
-17	.0	-3.9
-18	.0	-4.2
-19	.0	-6.4
-20	10.1	8.4
-21	14.0	16.0
-22	.0	-2.6
-23	12.6	15.6
-24	9.9	-12.2
	30ℓ̄	
-1	20.9	-19.5
-2	3.0	3.0
-3	20.8	-18.5
-4	24.3	-21.1
-5	13.9	-12.5
-6	12.9	-9.3
-7	12.7	-10.3
-8	26.7	30.0
-9	18.0	-16.1
-10	6.9	6.3
-11	15.6	-15.7
-12	25.6	-32.0
-13	7.2	-7.3
-14	5.3	-7.4
-15	.0	-5.0
-16	18.9	18.7
-17	4.4	-8.3
-18	.0	.8
-19	.0	-7.7
-20	7.3	-10.1
	40ℓ̄	
-1	15.7	12.3
-2	8.8	-6.6
-3	30.3	31.5
-4	9.2	7.8
-5	16.1	-13.3
-6	.0	.0
-7	23.5	-23.4
-8	8.0	-7.3
-9	.0	-.8
-10	4.7	-1.3
-11	.0	-2.5
-12	.0	-1.3
-13	.0	-3.0
-14	.0	-3.3
-15	.0	3.1
-16	.0	2.0
-17	10.3	-13.9
-18	.0	.7
-19	19.0	-21.1
	50ℓ̄	
-1	13.2	11.0
-2	.0	.9
-3	21.6	20.4
-4	15.5	-12.0
-5	10.7	8.8
-6	9.5	-8.5
-7	8.6	-6.9
-8	18.7	15.7
-9	16.4	15.0
-10	7.2	6.5
-11	25.1	27.5
-12	22.7	-20.4
-13	.0	1.3
-14	11.3	-10.5
-15	6.3	-7.8
-16	9.3	9.2
-17	9.7	10.3
-18	5.1	1.4
-19	7.5	11.8
-20	7.7	-8.1
	60ℓ̄	
-1	.0	1.3
-2	8.9	-7.5
-3	11.3	10.3
-4	29.4	31.2
-5	.0	1.6
-6	21.5	21.6
-7	.0	-3.9
-8	.0	-2.5
-9	.0	1.0
-10	.0	4.9
-11	.0	3.9
-12	6.0	7.4
-13	.0	5.1
-14	.0	3.3
-15	.0	5.8
-16	15.0	15.4
-17	.0	.6
-18	10.8	12.0
	70ℓ̄	
-1	.0	-1.2
-2	.0	-1.6
-3	6.7	7.0
-4	.0	1.0
-5	.0	-2.9
-6	.0	5.4
-7	24.6	-21.7
-8	.0	1.8
-9	.0	.6
-10	.0	1.1
-11	23.5	22.1
-15	19.3	-19.6
	80ℓ̄	
-2	26.9	-25.4
-3	13.8	-13.5
-4	.0	1.4
-5	.0	.3
-6	.0	2.5
-7	7.9	9.4
-8	14.8	-14.2
-9	4.7	-.7
-10	13.8	-12.7
-11	.0	-1.3
-12	8.9	-8.5
	90ℓ̄	
-1	.0	-3.1
-2	.0	-3.6
-3	.0	-1.7
-4	.0	2.7
-5	7.0	-6.6
-6	10.1	8.8
-7	12.5	-13.2
-8	10.3	-10.8
-9	5.2	-5.2
-10	16.1	-16.3
-11	.0	4.3
-12	.0	7.2
-13	.0	-3.3
-14	5.6	8.6
-15	8.1	-11.4
-16	8.2	-12.0
	100ℓ̄	
-7	7.8	10.2
	11.0ℓ̄	
-6	10.0	9.2
-7	10.0	11.1
	11ℓ	
3	30.8	-34.3
4	10.4	-6.6
5	26.6	-25.2
6	24.5	-27.7
7	5.9	-5.6
8	.0	.2
9	10.8	-10.3
10	3.1	3.2
11	12.5	-11.7
12	.0	-1.4
13	6.4	-7.5
14	6.8	6.3
15	11.7	-13.5
16	6.2	-6.9
17	10.3	-11.0
18	18.1	-18.8
19	.0	2.2
20	.0	2.8
21	.0	-.7
22	11.4	13.7
23	8.3	-11.3
	21ℓ	
0	17.8	-13.9
1	2.1	2.0
2	31.0	-25.1
3	13.1	-8.8
4	11.9	-8.3
5	6.7	-4.8
6	15.7	12.6
7	19.7	20.7
8	18.4	-18.4
9	15.4	12.7
10	27.4	-35.1
11	15.2	-13.3
12	.0	.7
13	.0	-3.1
14	14.1	13.0
15	16.6	16.9
16	14.3	-11.6
17	11.6	9.1
18	14.1	-14.5
19	.0	-1.1
20	14.4	-1.3
	31ℓ	
0	3.5	2.5
1	24.8	22.9
2	12.6	8.0
3	28.1	-29.1
4	.0	1.8
5	7.8	-6.4
6	.0	-.3
7	22.3	22.6
8	3.2	4.4
9	7.5	7.4
10	7.9	6.9
11	.0	3.2
12	8.7	7.2
13	4.0	5.3
14	6.0	6.8
15	9.0	-9.6
16	.0	4.3
17	.0	-1.9
18	.0	4.0
19	19.5	20.0
20	.0	7.7
21	.0	6.2
22	.0	8.5
23	13.3	-14.9
	41ℓ	
0	16.6	13.9
1	.0	-2.3
2	5.9	5.1
3	5.2	4.8
4	25.1	24.3
5	3.1	3.8
6	30.3	35.3
7	9.0	-7.6
8	3.5	-2.6
9	3.6	-1.9
10	13.8	-13.4
11	8.9	9.2
12	20.0	23.5
13	.0	1.7
14	22.3	26.9
	51ℓ	
0	17.3	-13.4
1	14.7	12.5
2	20.0	-19.7
3	17.9	-14.2
4	11.4	9.3
5	.0	2.1
6	9.6	7.5
7	16.3	16.9
8	10.6	-9.4
9	8.0	7.6
10	4.1	-5.2
11	4.3	4.7
12	6.3	-5.5
13	.0	2.8
14	10.9	-10.7
15	.0	-5.1
16	.0	1.1
17	.0	3.0
18	.0	3.6
19	12.9	14.3
20	11.7	-13.3
21	.0	1.8
22	12.0	-13.1
	61ℓ	
0	9.8	-9.3
1	3.7	-1.8
2	8.4	-7.8
3	11.1	11.7
4	.0	-1.7
5	.0	-1.0
6	.0	-2.1
7	24.9	-25.7
8	11.7	-11.9
9	.0	-4.0
10	12.0	-11.1
11	17.0	19.1
12	.0	.1
13	.0	-4.8
14	.0	.7
15	18.8	-21.1
	71ℓ	
0	20.9	-19.6
1	12.9	-10.0
2	19.5	-17.5
3	11.3	-7.3
4	18.4	15.5
5	10.8	-11.9
6	10.0	11.0
7	12.6	-10.6
8	4.7	-5.9
9	6.8	-6.2
10	.0	-1.5
11	7.2	-8.3
12	.0	-2.6
13	9.4	-8.5
14	.0	-3.7
15	.0	-3.9
16	10.0	11.0
17	.0	-4.5
18	.0	8.6
19	.0	-6.6
20	10.5	-11.6
	81ℓ	
0	.0	-2.3
1	.0	3.1
2	.0	2.3
3	9.5	10.6
4	8.3	-8.0
5	.0	-1.3
6	10.0	-8.8
7	12.5	-12.5
8	5.2	7.8
9	7.5	7.3
10	.0	4.8
11	18.5	20.1
12	8.0	-10.8
	91ℓ	
0	9.0	-8.1
1	10.4	11.8
2	5.2	-4.8
3	24.3	22.5
4	5.3	7.5
	10.1ℓ	
0	11.3	9.4
8	20.5	21.5
	01ℓ̄	
-5	20.8	24.2
-7	20.0	-21.5
-9	17.9	-17.6
-11	27.4	33.5
-13	24.4	25.6
-15	12.3	-12.8
-17	4.5	-3.8
-19	15.5	15.9
-21	9.5	9.8
	11ℓ̄	
-3	31.2	-31.5
-4	2.1	-1.6
-5	26.6	-28.5
-6	26.0	28.9
-7	7.4	-6.8
-8	.0	3.1
-9	8.8	-8.5
-10	5.4	-3.9
-11	11.4	-11.9
-12	.0	2.3
-13	7.3	-7.3
-14	5.5	-6.3
-15	10.8	-12.1
-16	.0	3.8
-17	12.4	-11.9
-18	17.9	19.9
-19	.0	1.0
-20	.0	1.2
-21	.0	1.3
-22	11.3	-14.4
-23	8.2	-10.0
-24	5.9	4.5
-25	.0	-7.4
-26	13.5	15.4
	21ℓ̄	
-1	3.0	-2.6
-2	30.4	-23.5
-3	7.5	5.1
-4	20.5	-17.5
-5	13.7	10.3
-6	15.4	11.8
-7	17.5	-15.1
-8	7.6	-6.7
-9	22.2	-20.0
-10	28.3	-37.6
-11	8.6	8.3
-12	11.3	-11.6
-13	8.4	9.5
-14	14.3	14.6
-15	12.5	-13.5
-16	7.6	-5.0
-17	10.3	-12.7
-18	15.3	-17.6
	31ℓ̄	
-1	42.6	43.7
-2	10.1	-7.5
-3	17.1	-13.0
-4	6.5	-5.0
-5	29.1	-23.6
-6	.0	.2
-7	17.8	15.0
-8	.0	-2.7
-9	17.2	14.2
-10	6.8	-6.0
-11	.0	1.6
-12	6.4	-6.8
-13	6.7	7.0
-14	8.2	-7.9
-15	.0	-4.6
-16	4.5	-5.9
-17	9.4	-11.4
-18	.0	-3.1
-19	11.6	12.3
-20	.0	-6.2
-21	12.6	16.1
-22	10.0	-9.2
-23	5.8	-10.3
-24	.0	-6.1
-25	6.0	-11.7
	41ℓ̄	
-1	.0	1.6
-2	8.4	7.3
-3	.0	.1
-4	9.9	8.3
-5	9.2	-6.9
-6	35.7	36.4
-7	.0	1.8
-8	21.3	22.7
-9	9.2	8.1
-10	17.8	-16.1
-11	3.8	-4.2
-12	3.9	.8
-13	8.2	-8.1
-14	27.1	31.7
-15	.0	2.7
-16	12.4	13.6
-17	.0	3.7
-18	7.2	-6.6
-19	.0	-3.1
-20	.0	2.5
-21	.0	-2.2
-22	5.8	6.5
	51ℓ̄	
-1	31.8	31.5
-2	22.7	21.3
-3	3.3	2.1
-4	14.7	11.9
-5	14.1	-11.9
-6	13.5	-12.1
-7	10.1	9.2
-8	.0	-.8
-9	13.7	14.2
-10	8.8	9.2
-11	4.0	6.3
-12	.0	3.5
-13	4.4	7.5
-14	6.4	9.1
-15	.0	.5
-16	7.0	9.1
-17	.0	-5.5
-18	.0	-4.8
-19	7.9	8.9
-20	.0	.3
-21	10.1	14.3
-22	11.8	16.4
	61ℓ̄	
-1	3.7	2.0
-2	10.1	-10.2
-3	.0	.1
-4	7.5	-7.7
-5	15.7	-14.5
-6	.0	.1
-7	6.8	5.9
-8	.0	-2.4
-9	25.5	26.8
-10	12.1	-12.6
-11	.0	-1.2
-12	11.2	-8.9
-13	17.7	-18.0
-14	.0	1.7
-15	8.8	9.2
-16	.0	.0
-17	16.4	19.2
	71ℓ̄	
-1	14.4	-14.9
-2	19.0	18.7
-3	9.3	-10.0
-4	16.8	16.3
-5	7.4	-7.2
-6	12.6	-14.5
-7	12.0	-11.9
-8	10.5	-9.9
-9	10.3	-10.8
-10	.0	3.6
-11	6.8	-6.4
-12	.0	-.3
-13	7.2	-8.1
-14	.0	4.2
-15	5.4	-8.4
-16	.0	4.7
-17	.0	-4.3
-18	10.0	-12.4
-19	.0	-4.5
-20	.0	-9.3
-21	.0	-6.5
-22	12.1	12.1
	81ℓ̄	
-1	.0	1.0
-2	.0	-2.5
-3	.0	-2.2
-4	4.7	3.2
-5	13.4	-13.1
-6	9.6	-7.2
-7	.0	-2.1
-8	9.9	-11.3
-9	13.4	13.7
-10	.0	5.5
-11	.0	-3.8
-12	7.6	6.5
-13	21.5	-20.7
-14	7.9	-10.1
-15	.0	-4.8
-16	8.2	-7.8
-17	5.9	6.5
	91ℓ̄	
-1	11.6	-11.8
-2	.0	5.1
-3	.0	3.3
-4	7.4	7.6
-5	23.0	22.5
-6	5.3	-3.8
-7	7.6	7.9
-8	7.7	-6.7
-17	10.4	12.7
	10.1ℓ̄	
-1	5.6	1.5
-2	9.8	9.0
-3	.0	-1.7
-4	15.0	14.1
-5	.0	-.2
-6	5.7	.7
-7	5.7	2.8
-8	5.8	-6.7
-9	.0	2.3
-10	15.5	15.1
-11	.0	1.2
-12	18.8	20.5
	11.1ℓ̄	
-1	13.3	-14.5
-2	.0	-2.3
-3	8.4	-7.0
-4	.0	-5.3
-5	8.4	11.3

The structures of the ditellurides of niobium and tantalum which have been worked out as part of this project, have similar metal–metal chains parallel to the *b* axis except that the chains are made of three rows of metal atoms rather than two. Details of this work are presented in a companion paper (Brown, 1966).

References

BUERGER, M. J. (1959). *Vector Space*. New York: John Wiley.

BROWN, B. E. (1966). *Acta Cryst.* **20**, 264.

BUSING, W. & LEVY, H. A. (1959). Oak Ridge National Laboratory Central Files, No. 59-4-37.

GELLER, S. (1961). *Acta Cryst.* **14**, 1026.

GOLDSCHMIDT, V. M. (1919). *Trans. Faraday Soc.* **25**, 279.

JELLINEK, F. (1961). *Nature, Lond.* **192**, 1065.

KNOP, O. & HARALDSEN, H. (1956). *Canad. J. Chem.* **34**, 1142.

MARINDER, B. & MAGNÉLI, A. (1957). *Acta Chem. Scand.* **11**, 1635.

MARINDER, B., DORM, E. & SELEBORG, M. (1962). *Acta Chem. Scand.* **16**, 293.

NITSCHE, R., BOLSTERLI, H. U. & LICHTENSTEIGER, M. (1961). *Phys. Chem. Solids*, **21**, 199.

PHILLIPS, D. C. (1954). *Acta Cryst.* **7**, 746.

PUOTINEN, D. & NEWNHAM, R. E. (1961). *Acta Cryst.* **14**, 691.

THOMAS, L. H. & UMEDA, K. (1957). *J. Chem. Phys.* **26**, 293.

Acta Cryst. (1966). **20**, 274

The Crystal Structure of the Strontium and Lead Tetraborates, $SrO.2B_2O_3$ and $PbO.2B_2O_3$

BY A. PERLOFF AND S. BLOCK

National Bureau of Standards, Washington, D.C., U.S.A.

(*Received* 29 *December* 1964 *and in revised form* 3 *June* 1965)

$SrO.2B_2O_3$ and $PbO.2B_2O_3$ are isostructural. These compounds crystallize in the orthorhombic system, $P2_1nm$, with two formula units in a cell of dimensions $a=4{\cdot}237$, $b=4{\cdot}431$, $c=10{\cdot}706$ Å for $SrO.2B_2O_3$, and $a=4{\cdot}244$, $b=4{\cdot}457$, $c=10{\cdot}840$ Å for $PbO.2B_2O_3$. A detailed structure analysis was carried out for the strontium compound only.

The structure was solved by conventional Patterson and electron-density syntheses utilizing the heavy atom to establish the initial phases. Least-squares refinement on three-dimensional data yielded a residual $R=7{\cdot}1$ %.

The results reveal an unusual type of borate framework. All boron atoms are tetrahedrally coordinated. The unusual feature is the occurrence of an oxygen atom common to three tetrahedra.

Although the tetrahedra form a three-dimensional network by corner sharing, the borate network gives the appearance of a layer-like structure because there are comparatively few links in the **c** direction. The layers can be described in terms of chains (parallel to **a**) of six-membered rings having B–O edges in common. These chains are joined by non-ring oxygens to form layers parallel to the *a b* plane.

The Sr coordination is not clearly defined. There are nine nearest-neighbor oxygen atoms at distances ranging from 2·52 to 2·84 Å. There are six more oxygen atoms at 3·04 to 3·20 Å which could conceivably be considered as part of the Sr coordination sphere.

Introduction

In previous studies (Weir & Schroeder, 1964; Block, Perloff & Weir, 1964) on a series of $M^{II}O.2B_2O_3$ compounds (M = Ca, Ba, Zn, Sr, Pb) it has been observed that the Sr and Pb borates are isostructural with each other, but apparently of a structure type completely different from the others. It was also noted that the Sr and Pb borates had an unusually dense structure compared with most known borates, which suggested the possibility of a new borate structure type. A single-crystal X-ray structure analysis was undertaken on $SrO.2B_2O_3$ to investigate this possibility. Only the Sr compound is reported in detail, but the structure is valid for the Pb compound.

Cell and space group

The cell dimensions and diffraction aspect have been previously reported by Block, Perloff & Weir (1964) with axial designations interchanged from those used in this work. The present structure is based on the following orthorhombic cell data* for $SrO.2B_2O_3$:

$a=4{\cdot}237\pm0{\cdot}004$ Å	Space group $P2_1nm$
$b=4{\cdot}431\pm0{\cdot}004$	$Z=2$
$c=10{\cdot}706\pm0{\cdot}010$	ϱ (calc.) $=4{\cdot}01$

Systematic extinctions: $h0l$, $h+l=2n+1$

---

* The uncertainties quoted on the cell dimensions are standard deviations based on least-squares refinement of powder pattern data.